Ionization and protonation of NaC3: A theoretical study

ARTICLE *in* JOURNAL OF MOLECULAR STRUCTURE THEOCHEM · JULY 2003

Impact Factor: 1.37 · DOI: 10.1016/S0166-1280(03)00169-6

3 AUTHORS:

Pilar Redondo
Universidad de Valladolid
91 PUBLICATIONS **969** CITATIONS
SEE PROFILE

Carmen Barrientos
Universidad de Valladolid
124 PUBLICATIONS **1,359** CITATIONS
SEE PROFILE

Antonio Largo
Universidad de Valladolid
135 PUBLICATIONS **1,620** CITATIONS
SEE PROFILE

ELSEVIER

Journal of Molecular Structure (Theochem) 630 (2003) 59–73

THEO CHEM

www.elsevier.com/locate/theochem

Ionization and protonation of NaC_3: a theoretical study

Pilar Redondo*, Carmen Barrientos, Antonio Largo

Departamento de Química Física, Facultad de Ciencias, Universidad de Valladolid, 47005 Valladolid, Spain

Received 7 August 2002; accepted 18 November 2002

Abstract

A theoretical study of the NaC_3^+ and NaC_3H^+ systems has been carried out. Predictions have been made for some of the molecular properties, which could help in their possible experimental detection. The predicted global minimum for NaC_3^+ is the linear isomer **1s** ($^1\Sigma$). The lowest-lying triplet state is a three-membered ring **3t** ($^3B_2$), lying about 27.1 kcal/mol higher in energy than the predicted global minimum at the G2(P) level. In the case of NaC_3H^+, there are two isomers that lie close in energy: a linear species, **1d** ($^2\Pi$), and a three-membered ring, **4d** ($^2A'$). The most reliable levels of theory employed predict that **1d** ($^2\Pi$) is the global minimum, whereas **4d** ($^2A'$) is predicted to lie 5.3 kcal/mol higher in energy at the G2(P) level. In any case it seems that both structures could be accessible to experimental detection. Low ionization potential and high proton affinities are obtained for the most stable NaC_3 isomers. Therefore, if present in the interstellar medium, NaC_3 should be easily ionized and would react quite easily to give the protonated species.

Keywords: Ab initio; Density functional; Astrochemical molecules; Molecular properties; Sodium compounds; Ionization potential; Proton affinity

1. Introduction

The gas-phase chemistry of refractory elements, particularly aluminium, magnesium and sodium, has received much attention in recent years, in part due to their potential interest in astrochemistry. In fact a number of molecules containing these metals has already been detected in space. To date, MgNC [1], MgCN [2], AlCl [3], AlF [3], AlNC [4], NaCN [5] and NaCl [3] have been detected via radioastronomical observation. In contrast to the chemistry of non-metallic elements (H, C, N, O, Si and S) in dense interstellar clouds, the chemical evolution of the abundant metals Na, Mg, Al, K, Ca, Fe and Ni within such objects has received very little attention.

In last years, there have been numerous theoretical and experimental investigations devoted to determine the stability of various sizes and compositions of metal carbides as SiC_2 [6,7], SiC_3 [8,9], SiC_4 [10], SiC_5 [8], SiC_6 [10], AlC_2 [11–16], AlC_3 [17,18], MgC_2 [15,19,20] and MgC_3 [21,22]. A number of binary compounds corresponding to the general formula XC_n (X = Si, S and $n = 2, 3$) have been detected in space, and it is expected that new binary carbides could been detected in interstellar medium. Metal carbides are also interesting for solid-state chemistry, since they are the basic structural units of

* Corresponding author. Fax: +34-983-42320.
E-mail address: predondo@qf.uva.es (P. Redondo).

0166-1280/03/$ - see front matter © 2003 Elsevier Science B.V. All rights reserved.
doi:10.1016/S0166-1280(03)00169-6

new materials with interesting potential applications. Concerning sodium carbides, NaC_2 presents a cyclic $^1A_1$ ground state [23], and recently, we have carried out a theoretical study of the NaC_3 species [24]. According to our results there are three species lying quite close in energy: a linear isomer ($^2\Pi$), a rhombic four-membered ring ($^2A_1$), and a T-shape species ($^2A_2$). The linear isomer seems to be the best candidate for the global minimum, although the rhombic isomer and the T-shape species are predicted to lie only 1.5 and 1.7 kcal/mol, respectively, higher in energy, and therefore, they could also be accessible to experimental detection. Neutral and protonated NaC_3H isomers have also be studied at the G2 level of theory [25,26]. The global minimum for both systems, NaC_3H and $NaC_3H_2^+$, is a singlet C_3-ring-containing structure.

In the present work, we performed a theoretical study of the cationic and protonated derivatives of NaC_3. It is interesting to obtain information about molecular ions because ion-molecule chemistry plays an important role in the production of interstellar molecules, as well as in general gas-phase chemistry. This article provides information about the structures and stabilities of NaC_3^+ and NaC_3H^+ species, and allows an estimate of two important properties, the ionization potential and proton affinity of NaC_3. In addition NaC_3H^+ system is interesting since it could be the precursor in the interstellar medium of neutral NaC_3 upon dissociative recombination. To characterize the chemical nature of the bonding in these cluster ions, we have also carried out a topological analysis of the electronic charge density.

2. Computational methods

The same methods employed in our previous study on NaC_3 have been employed. The geometries of the different NaC_3 and NaC_3H^+ species have been obtained at the second-order Møller–Plesset level with the triple-split-valence polarized 6-311G(d,p) basis set [27], including all electrons in the calculation, which is denoted MP2(full)/6-311G(d,p), and also using density functional theory (DFT). In particular, for the DFT calculations we selected the Becke's hybrid three-parameter functional combined with the Lee–Yang–Parr non-local correlation functional B3LYP [28] with the 6-311G(d,p) basis set.

Harmonic vibrational frequencies were computed on each optimized structure at its corresponding level of theory. This enables us to assess the nature of stationary points, to verify that they correspond to true minima on the potential surface, and also to estimate the zero-point vibrational energy (ZPVE) correction.

To compute accurate relative energies, we have employed higher-level theoretical methods. The G1 and G2 methods [29] were employed and, since we are dealing with open-shell states, spin-contamination may affect the convergence of the MP series, approximate projected MP values were employed to compute electronic energies. These results will be denoted as G1(P) and G2(P). In addition, we have also carried out CCSD(T) calculations (coupled-cluster single and double excitation model augmented with a non-iterative triple excitation correction) [30] with the B3LYP geometry. In these calculations we employed a basis set with additional polarization functions, namely the 6-311G(2df,p) basis set. The reliability of single-reference-based methods has been tested through the so-called $T1$-Diagnostic [31]. In all cases, $T1$ values are well below the critical value.

In most of its compounds, and specially within cations, the sodium atom can be treated largely as Na^+. Since Na^+ is isoelectronic with F^- and Ne, it seems appropriate to apply a similar electron correlation treatment to all three. Thus the 2s, $2p_x$, $2p_y$ and $2p_z$ orbitals can be considered as the valence shell for Na^+. Therefore, we have included these orbitals in the G2 and CCSD(T) calculations. Following Petrie [32] we term these calculations as G2(thaw/MP2) and CCSD(T,raw), respectively. In the case of G2(thaw/MP2) calculations an additional calibration constant is included to make these values comparable with standard G2 results [32].

All these calculations were carried out with the GAUSSIAN-98 program package [33].

The nature of bonding for the different NaC_3^+ and NaC_3H^+ species was characterized by using Bader's topological analysis of the electronic charge density [34]. Extrema or critical points in the one electron density $\rho(r)$ were identified, through its gradient vector field $\nabla\rho(r)$, and classified according to rank and curvature. A $(3, -1)$ critical point has a minimum value of $\rho(r)$ along the line linking nuclei and

a maximum along the interatomic surfaces and represents a 'bond critical point' (three non-zero eigenvalues, λ_i, of the Hessian of $\rho(r)$, two of them being negative and the other one positive). 'Ring critical points' corresponds to (3, + 1) points ($\rho(r)$ is a minimum in two directions and a maximum in one direction). In addition, the Laplacian of the charge density, $\nabla^2\rho(r)$, determines where electronic charge is locally concentrated, ($\nabla^2\rho(r) < 0$), and where it is locally depleted ($\nabla^2\rho(r) > 0$). The two negative curvatures, λ_1 and λ_2, of a bond critical point define the ellipticity of the bond, ε ($\varepsilon = (\lambda_1/\lambda_2) - 1$, where λ_2 corresponds to the softest mode) which provides a measure of the extent to which charge is preferentially accumulated in a given plane. The total energy density, $H(r)$, is the sum of the potential and kinetic energy density at a critical point and characterized a bond as covalent ($H(r) < 0$) or ionic ($H(r) > 0$) [35].

These calculations were performed with the MORPHY program [36], using both the MP2/6-311G* and B3LYP/6-311G* wave functions.

3. Results and discussion

3.1. NaC_3^+ species

We have searched for different isomers on both the singlet and triplet NaC_3^+ potential surfaces. Their optimized geometries at the MP2(full)/6-311G(d) and B3LYP/6-311G(d) levels are shown in Fig. 1. The corresponding Mulliken population charges are also reported. Other isomers, such as a linear isomer with the sodium atom in a central position, were also considered but are not presented since they lie much higher in energy. In general, there are no important differences between the MP2 and B3LYP geometrical parameters, shown in Fig. 1, except in the case of isomer **2s** ($^1A_1$), where the C_1–C_3 bond distance is lengthened by 0.273 Å when passing from MP2 to B3LYP. In Table 1 we report the vibrational frequencies and the dipole moments (taking the center of mass as origin), at the MP2(full)/6-311G(d) and B3LYP/6-311G(d) levels, for the different NaC_3^+ species, and the results of the topological analysis of the electronic density are given in Table 2. We will briefly describe the most important features of the different NaC_3^+ species.

Structure **1** corresponds to the linear NaC_3^+ isomer. The lowest-lying singlet ($^1\Sigma$), denoted as **1s**, corresponds to the following electronic configuration:

$$\{\text{core}\}(7\sigma)^2(8\sigma)^2(9\sigma)^2(2\pi)^4(10\sigma)^2 \quad (1)$$

Isomer **1s** can be viewed as a sodium cation bonded to a terminal carbon atom of a linear C_3 system. The C–C bond distances close to typical double-bond length, and Na–C σ bond has a dative character from sodium toward carbon, as a consequence of the following valence-bond structure:

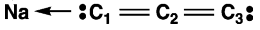

with the positive charge located at the sodium atom (Fig. 1). Isomer **1s** is a true minimum on both MP2 and B3LYP surfaces since all its frequencies are real (see Table 1). The IR intensities suggest that the infrared spectrum would be dominated by the ν_1 (C–C stretching) frequency. The dipole moment of structure **1s** is very high, as a consequence of the positive charge supported by sodium atom.

On the other hand the lowest-lying open-chain structure on the triplet surface ($^3\Pi$), is a linear species, namely **1t**, which results from electronic configuration (1) upon a $10\sigma \rightarrow 3\pi$ excitation. In this structure, one of the unpaired electrons is located at the C_3 atom and the other one is almost equally distributed between C_1 and C_3, whereas the positive charge mainly resides at the sodium atom. These characteristics are compatible with a description of this species in terms of the following two dominant valence-bond structures:

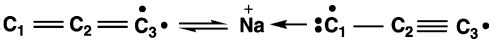

This description is also consistent with the linearity of this molecule and with the fact that the C_2–C_3 length is shorter than the C_1–C_2 one. This linear triplet isomer has all real frequencies and therefore corresponds to a true minimum on the triplet potential surface. The IR intensities suggest that the IR spectrum would be dominated by the ν_1 frequency.

Isomer **2** corresponds to a rhombic structure where the sodium atom is bonded to the side of a cyclic C_3 unit. The electronic configuration of the singlet **2s** ($^1A_1$) species is the following:

$$\{\text{core}\}(6a_1)^2(3b_2)^2(7a_1)^2(2b_1)^2(8a_1)^2(4b_2)^2 \quad (2)$$

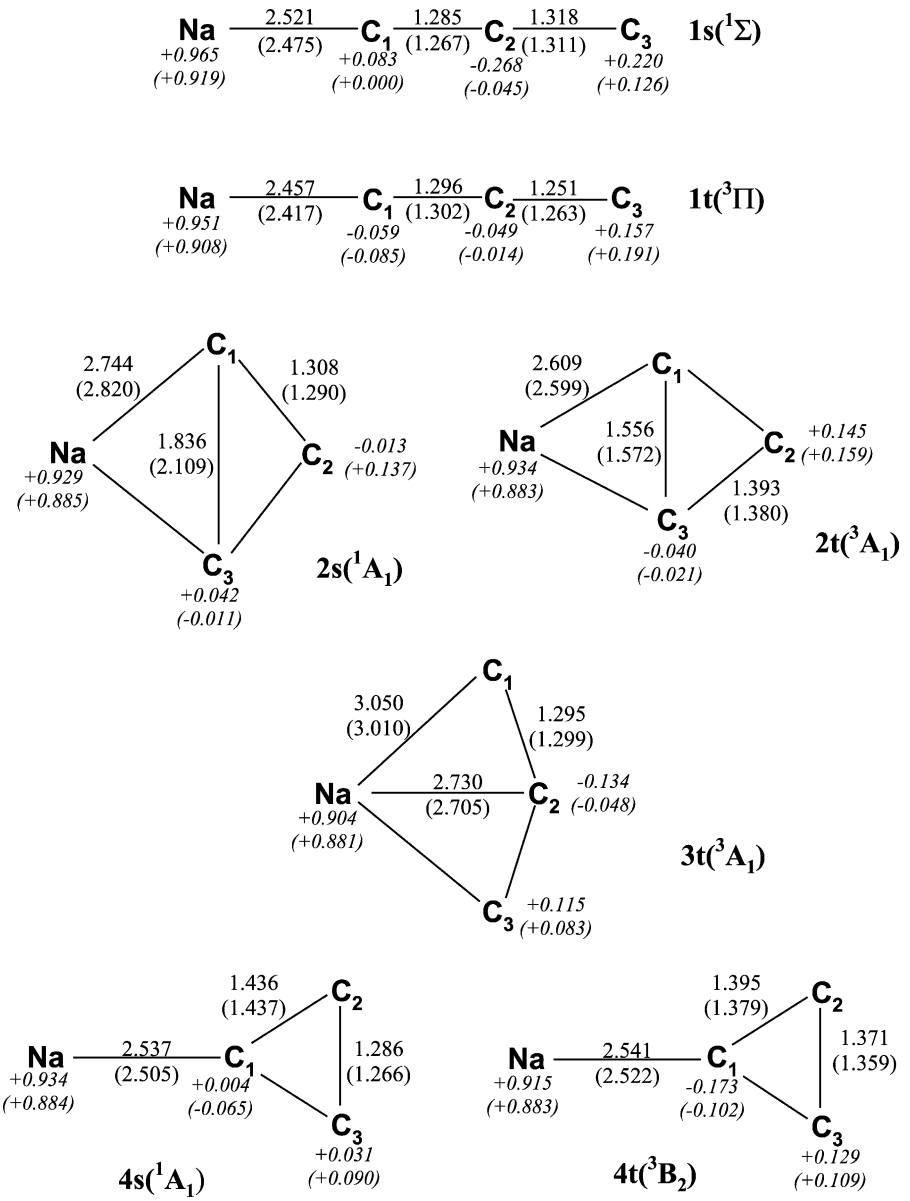

Fig. 1. MP2(full)/6-311G(d) and B3LYP/6-311G(d) (in parentheses) optimized geometries for the different NaC_3^+ isomers. Distances are given in angstroms and angles in degrees. Effective Mulliken charges on atom (shown in italics) computed using HF/6-311G(d) and B3LYP/6-311G(d) (in parentheses) densities.

This state is obtained from configuration of NaC_3 ($^2A_1$) simply by the loss of the unpaired $9a_1$ electron [19], and has an imaginary frequency (b_2 symmetry) at both MP2 and B3LYP levels of theory. All our attempts to obtain a true minimum at both levels in C_s symmetry finally collapse into the structure **1s**. In addition, for structure **2s** we have carried out a geometrical optimization at the CCSD(T)/6-31G(d) level, the geometrical parameters are very similar to those at the MP2 = full/6-311G(d) level, and

Table 1
MP2(full)/6-311G(d) and B3LYP/6-311G(d) (in parentheses) vibrational frequencies, in cm^{-1}, ZPV energies, in kcal/mol, and dipole moments, in Debyes, for the different NaC_3^+ species

	1s ($^1\Sigma$)	**1t** ($^3\Pi$)	**2s** ($^1A_1$)	**2t** ($^3A_1$)	**3t** ($^3A_1$)	**4s** ($^1A_1$)	**4t** ($^3B_2$)
$\nu_1(a_1,\sigma)$	2166 (2178)	1775 (1868)	1645 (1568)	1539 (1546)	1295 (1197)	1776 (1835)	1552 (1614)
$\nu_2(a_1,\sigma)$	1212 (1250)	1326 (1283)	320 (185)	834 (780)	488 (403)	1376 (1368)	1055 (1135)
$\nu_3(a_1,\sigma)$	208 (216)	232 (241)	166 (138)	344 (203)	151 (148)	208 (208)	199 (195)
$\nu_4(b_2,\pi)$	283 (261)	458 (416); 392 (349)	1681 (1906)	1065 (1380)	1945 (431i)	150 (151)	1181 (1158)
$\nu_5(b_1,\pi)$	93 (76)	126 (117); 108 (109)	185 (176)	210 (172)	305 (217)	192 (191)	182 (179)
$\nu_6(b_2)$			94i (133i)	154 (159)	301 (458)	991i (845i)	124 (120)
ZPVE	6.20 (6.17)	6.32 (6.27)	5.71 (5.68)	5.93 (6.06)	6.41 (3.46)	5.29 (5.37)	6.14 (6.29)
μ	8.283 (8.038)	5.831 (5.289)	5.708 (5.567)	4.678 (5.038)	6.701 (6.508)	6.945 (6.381)	6.227 (6.993)

the vibrational analysis also shows an imaginary frequency of b_2 symmetry. Consequently, this structure should be considered as a transition state at all levels of theory, and the differences in the geometrical structure (mainly in C_1-C_2 bond distance) are not of direct experimental interest. The topological analysis of the electronic charge density (Table 2) suggests that there is no transannular C_1-C_3 bond, and that this species can be described as a four-membered ring.

Table 2
Critical point data for NaC_3^+ species, using the MP2(full)/6-311(d) and B3LYP/6-311G(d) (in parentheses) wave functions

Structure	Type	R^a (Å)	R^b (Å)	$\rho(r)$ (a.u.)	$\nabla^2\rho(r)$ (a.u.)	ε	$-H(r)$ (a.u.)
1s	Na–C_1 bond	2.521 (2.475)	2.521 (2.475)	0.0179 (0.0201)	0.0930 (0.1021)	0.0000 (0.0000)	0.0194 (0.0214)
	C_1-C_2 bond	1.285 (1.267)	1.285 (1.267)	0.3722 (0.3908)	−1.2286 (−1.3371)	0.0000 (0.0000)	0.1761 (0.1781)
	C_2-C_3 bond	1.318 (1.311)	1.318 (1.311)	0.3586 (0.3688)	−1.2214 (−1.2692)	0.0000 (0.0000)	0.1440 (0.1352)
1t	Na–C_1 bond	2.457 (2.417)	2.457 (2.417)	0.0206 (0.0226)	0.1097 (0.1167)	0.0449 (0.0500)	0.0232 (0.0248)
	C_1-C_2 bond	1.296 (1.302)	1.296 (1.302)	0.3599 (0.3580)	−1.1880 (−1.1562)	0.2656 (0.1976)	0.1677 (0.1552)
	C_2-C_3 bond	1.251 (1.263)	1.251 (1.263)	0.3658 (0.3604)	−1.0702 (−1.0441)	0.0288 (0.0592)	0.2322 (0.2027)
2s	Na–C_1 bond	2.744 (2.820)	2.775 (2.858)	0.0089 (0.0074)	0.0458 (0.0343)	0.5681 (0.4740)	0.0092 (0.0068)
	C_1-C_2 bond	1.308 (1.290)	1.313 (1.294)	0.3495 (0.3699)	−1.0132 (−1.1880)	0.0936 (0.0287)	0.1846 (0.1717)
	$NaC_1C_2C_3$ ring			0.0083 (0.0067)	0.0429 (0.0302)		0.0086 (0.0060)
2t	Na–C_1 bond	2.609 (2.599)	2.647 (2.633)	0.0131 (0.0136)	0.0770 (0.0763)	4.7802 (4.0498)	0.0155 (0.0154)
	C_1-C_2 bond	1.393 (1.380)	1.414 (1.398)	0.2943 (0.3053)	−0.7049 (−0.7717)	0.0333 (0.0344)	0.1360 (0.1310)
	$NaC_1C_2C_3$ ring			0.0130 (0.0136)	0.0778 (0.0771)		0.0155 (0.0154)
3t	Na–C_2 bond	2.730 (2.705)	2.730 (2.705)	0.0098 (0.0103)	0.0465 (0.0474)	0.5913 (0.4535)	0.0095 (0.0097)
	C_1-C_2 bond	1.295 (1.299)	1.295 (1.299)	0.3417 (0.3401)	−1.0026 (−0.9783)	0.1840 (0.1360)	0.1857 (0.1674)
4s	Na–C_1 bond	2.537 (2.505)	2.537 (2.505)	0.0179 (0.0194)	0.0901 (0.0947)	0.0099 (0.0137)	0.0189 (0.0199)
	C_1-C_3 bond	1.436 (1.437)	1.603 (1.799)	0.2659 (0.2700)	−0.1221 (−0.0114)	4.6821 (29.6784)	0.2070 (0.2133)
	C_2-C_3 bond	1.286 (1.266)	1.292 (1.272)	0.3862 (0.4083)	−1.1924 (−1.3769)	0.1646 (0.1486)	0.2152 (0.2131)
	$C_1C_2C_3$ ring			0.2648 (0.2700)	0.0301 (0.0151)		0.2279 (0.2158)
4t	Na–C_1 bond	2.541 (2.522)	2.541 (2.522)	0.0166 (0.0175)	0.0828 (0.0831)	0.0141 (0.0123)	0.0173 (0.0175)
	C_1-C_3 bond	1.395 (1.379)	1.402 (1.382)	0.2958 (0.3039)	−0.4944 (−0.5457)	0.7168 (0.6431)	0.1875 (0.1845)
	C_2-C_3 bond	1.371 (1.359)	1.380 (1.360)	0.2805 (0.2970)	−0.3414 (−0.4825)	1.4500 (0.8399)	0.2104 (0.1991)
	$C_1C_2C_3$ ring			0.2709 (0.2764)	0.0370 (0.0996)		0.2352 (0.2444)

[a] Bond length.
[b] Bond path length.

The triplet state ($^3A_1$) for structure **2**, namely **2t**, results from $8a_1 \rightarrow 9a_1$ promotion. One of the unpaired electrons is mainly located at the C_2 atom and the other one is almost equally distributed between C_1 and C_3, and the sodium atom bears the positive charge as in its singlet equivalent. For the triplet state C_1-C_3 distance suggests the possibility of a trans-annular bonding. However, the topological analysis shows that there is no trans-annular C_1-C_3 bond, and therefore **2t**, as **2s**, should be described as a truly four-membered ring. As can be seen in Table 1 structure **2t** is a true minimum on the NaC_3^+ triplet potential surface at both levels of theory and has very high dipole moments of 4.678 D at the MP2 level.

For structure **2**, we have also located another triplet state, $^3B_2$, resulting from $4b_2 \rightarrow 9a_1$ excitation. This state is predicted to lie lower in energy than $^3A_1$. However, this state has an imaginary frequency (b_2 symmetry), at both MP2 and B3LYP levels and should be considered as the transition state for the degenerate rearrangement of isomer **4t**.

Structure **3** may be viewed as the result of the side interaction of a sodium cation with a cuasilinear C_3 unit. The lowest-lying triplet state, $^3A_1$, has a planar C_{2v} structure with the following electronic configuration

$$\{\text{core}\}(6a_1)^2(3b_2)^2(7a_1)^2(8a_1)^2(2b_1)^2(4b_2)^1(5b_2)^1 \quad (3)$$

where the two unpaired electrons are essentially located at the C_1 and C_3 carbon atoms and the sodium atom bears the positive charge. The topological analysis shows that for **3t** there is only $Na-C_2$ bond and no peripheral Na–C bonding, according with the fact that trans-annular distance is shorter than the peripheral distances, and therefore this isomer has in fact a T-shape structure. As can be seen in Table **3t** is a true minimum at the MP2 level but has an imaginary frequency (b_2 normal mode) at the B3LYP level.

We also searched for the corresponding singlet state, **3s**, but all our attempts collapsed into structure **2s**. Electronic configuration of isomer **2s** is also obtained from NaC_3 ($^2A_2$), corresponding to a T-shape structure, simply by the loss of the unpaired $1a_2$ electron [24].

Structure **4** can be viewed as the result of the interaction of a sodium cation with a cyclic C_3 unit to an apex. The singlet state for this structure $^1A_1$, denoted as **4s**, corresponds to the following electronic configuration

$$\{\text{core}\}(6a_1)^2(7a_1)^2(3b_2)^2(2b_1)^2(8a_1)^2(9a_1)^2 \quad (4)$$

and has an imaginary frequency (b_2 symmetry) at both MP2 and B3LYP levels of theory. All our attempts to obtain a true minimum in C_s symmetry finally collapsed into the structure **1s**. Consequently, structure **4s** should be in fact considered as a transition state.

The lowest-lying triplet state corresponding to structure **4**, denoted as **4t**, is generated from Eq. (4) by the electron excitation $9a_1 \rightarrow 4b_2$. The two unpaired electrons are mainly located at the C_2 and C_3 atoms and the sodium atom bears the positive charge. As can be seen in Table 1, this state has all its frequencies real at both levels of theory. The IR spectrum would be dominated by the ν_2 frequency. In contrast to the neutral **4d** ($^2A'$) isomer [24], the topological analysis of the electronic charge density for **4s** and **4t** isomers reveals that both can be described as truly three-membered rings.

The results of the topological analysis of the electronic charge density (Table 2), show that all Na–C bond correspond to closed-shell interactions, because they have small values of the electronic charge density at the bond critical point, $\rho(r)$, and are characterized by positive values for the Laplacian of the electronic charge density, $\nabla^2\rho(r)$. However, $H(r)$ is slightly positive. This means that all Na–C bonds should be classified as closed-shell interactions, corresponding essentially to electrostatic bonds with a small degree of covalent dative character. This is consistent with the positive partial electric charge of the sodium atom provided by Mulliken population analysis (Fig. 1). The highest value of $\rho(r)$ for the sodium carbon bonds is found for the $Na-C_1$ of isomer **1t**, whereas for C–C bonds the highest values of $\rho(r)$ are observed for C_2-C_3 bond of **4s** and **1t** isomers, and C_1-C_2 bond of **1s** isomer. These values correspond to the shortest Na–C and C–C bonds, respectively. From the values of bond path lengths, it can be seen that bonds are only slightly curved. The exceptions are $Na-C_1$ and C_1-C_3 bonds in structures **2t** and **4s**, respectively. In addition, these bonds show some characteristics of topological instability, because

the ellipticity values are somewhat high and the values of $\rho(r)$ are close to that of the ring critical points.

The relative energies of the different NaC_3^+ species at different levels of theory are shown in Table 3. We also provide the S^2 expectation value for the HF/6-311G(d) wave functions for triplets. In the case of B3LYP/6-311G(d) calculations S^2 values are very close to the exact value. As a general trend it can be seen in Table 3, that for this system there is a very good agreement between the G2 (G2(P) for triplet states) and CCSD(T) results, with discrepancies less than 2 kcal/mol, except for **1t** isomer. This difference can be related to the fact that this isomer has the highest spin-contaminated wave function. This agreement gives further support to the reliability of our predictions. Inclusion of 2s, $2p_x$, $2p_y$ and $2p_z$ orbitals for sodium in the G2 and CCSD(T) calculations (denoted as G2(thaw/MP2) and CCSD(T,raw), respectively) does not significantly modify their results. Also there is an excellent agreement between B3LYP values and G2(P), the largest discrepancy is observed for **4s** isomer (5 kcal/mol).

It is readily seen that at all levels of theory, the most stable species is the linear isomer in its singlet state, structure **1s**. The other two singlet states, **2s** and **4s**, lie higher in energy (11.1 and 22.2 kcal/mol above the **1s** at the G2(P) level, respectively), and we must remember that they are not true minima on the singlet potential surface. The relative energy order is reversed for the triplet isomers. The lowest-lying triplet state is **4t** and lies about 27.1 kcal/mol above **1s** at the G2(P) level, followed for the linear triplet **1t**, by just 17.5 kcal/mol. **3t** and **2t** are the less stable structures considered in this work at all levels of theory.

We have found the same stability order that in the neutral NaC_3 system [24], although the energy difference between the low-lying NaC_3^+ is higher than for the neutral analogue. As in the case of neutral NaC_3 system, the ionized NaC_3^+ species should be considered closer in behavior to AlC_3^+ [37] rather than to MgC_3^+ [38]. In addition, NaC_3^+ system shows the same stability order than C_3Cl^+ species [39].

We have also computed the dissociation energies for the different NaC_3^+ species in order to study their stability. The dissociation energy of the NaC_3^+ linear isomer, **1s**, into $Na^+ + C_3(^1\Sigma)$ has a value of 17.5 and 17.6 kcal/mol at the G2(thaw/MP2) and CCSD(T,raw) levels, respectively. For the lowest-lying triplet state, **4t**, we have obtained a value of 41.4(40.1) kcal/mol (G2(thaw/MP2) and

Table 3
Relative energies (kcal/mol) for the NaC_3^+ isomers at different levels of theory

	1s	**1t**	**2s**	**2t**	**3t**	**4s**	**4t**
MP2(full)/6-31G(d) geometry[a]							
MP2(full)/6-31(d)	0.0	61.1	9.9	75.1	60.8	21.8	25.3
G1	0.0	51.1	12.0	74.7	61.5	23.7	30.7
G2	0.0	50.3	11.1	72.5	60.6	22.2	28.3
G2(thaw/MP2)	0.0	50.1	11.2	72.4	60.9	22.3	28.4
G1(P)	0.0	41.4	12.0	72.3	56.4	23.7	29.5
G2(P)	0.0	40.7	11.1	70.1	55.6	22.2	27.1
B3LYP/6-311G(d) geometry[b]							
B3LYP/6-311G(d)	0.0	43.3	12.8	68.7	58.5	27.2	24.1
CCSD(T)/6-311G(2df)	0.0	47.1	10.0	70.1	56.7	23.3	26.1
CCSD(T,raw)/6-311G(2df)	0.0	47.0	10.3	70.0	56.9	23.4	26.3
MP2(full)/6-311G(d) geometry[c]							
MP2(full)/6-311G(d)	0.0	62.6	10.1	75.3	62.8	22.0	25.6
$\langle S^2 \rangle$		2.577		2.075	2.202		2.029

[a] Including ΔZPVE at the HF/6-31G(d) level scaled by 0.893.
[b] Including ΔZPVE at the B3LYP/6-311G(d) level.
[c] Including ΔZPVE at the MP2(full)/6-311G(d) level.

CCSD(T,raw) in parentheses) corresponding to this dissociation into $Na^+ + C_3(^3A_1)$. The dissociation energy of the other isomers can be easily estimated using the relative energies shown in Table 3.

The present calculations for NaC_3^+ allow an estimate of the adiabatic ionization potentials for NaC_3 isomers. In Table 4 we show the adiabatic ionization potentials at different levels of theory. As can be seen, there are only small differences in the computed ionization potentials at different levels of theory. The two most reliable methods of calculation, G2(thaw/MP2) and CCSD(T,raw), provide very similar ionization potentials, the largest discrepancy is observed for **2d** (0.12 eV). The values provided for the different NaC_3 isomers are very close. It is also worth noting that all ionization potentials are very small, and therefore these species should be easily ionized if they are present in interstellar media.

3.2. NaC_3H^+ species

We have searched for possible minima on both the doublet and quartet surfaces of NaC_3H^+. As in our previous study on NaC_3 [24] all quartet states are found to lie much higher in energy than the corresponding doublets, therefore, except in the case of structure **3**, only the doublet states will be discussed. Isomer **3** is not located on the doublet surface, and we report the results corresponding to the quartet state. Species obtained upon protonation of NaC_3 isomers at the sodium atom are much less stable and therefore will not be discussed. The optimized geometries at the MP2(full)/6-311G(d,p) and B3LYP/6-311G(d,p) levels are shown in Fig. 2. The corresponding Mulliken population charges obtained at the HF/6-311G(d,p) and B3LYP/6-311G(d,p) levels are also shown. In Table 5 we report the vibrational frequencies and the dipole moments, whereas the results of the topological analysis of the electronic charge density are given in Table 6.

Structure **1** corresponds to the linear NaC_3H^+ isomer. It can be viewed as the protonated derivative of the doublet open-chain NaC_3 species. The lowest-lying doublet ($^2\Pi$), denoted as **1d**, corresponds to the following electronic configuration:

$$\{\text{core}\}(7\sigma)^2(8\sigma)^2(9\sigma)^2(10\sigma)^2(2\pi)^4(3\pi)^1 \quad (5)$$

The unpaired electron is almost equally distributed between C_1 and C_3 carbon atoms and the positive charge is located at the sodium atom, as a

Table 4
Ionization potentials (eV) and proton affinity (kcal/mol) of the NaC_3 species at different levels of theory

	1d($^2\Pi$)		**2d**($^2A_1$)		**3d**($^2A_2$)		**4d**($^2A'$)	
	IP	PA	IP	PA	IP	PA	IP	PA
MP2(full)/6-31G(d) geometry[a]								
MP2(full)/6-31(d)	5.31	260.5	6.51	246.8	5.82	260.0	6.54	267.1
G1	6.21	259.9	6.78	244.8	6.70	259.7	6.92	263.7
G2	6.20	257.9	6.79	245.7	6.64	260.0	6.89	264.9
G2(thaw/MP2)	6.25	256.9	6.86	244.2	6.70	259.0	6.95	263.9
G1(P)	6.43	258.8	6.83	245.0	6.89	261.5	6.96	263.7
G2(P)	6.42	259.8	6.84	245.8	6.83	262.8	6.94	264.8
B3LYP/6-311G(d) geometry[b]								
B3LYP/6-311G(d)	6.56	259.9	7.05	246.8	6.90	266.3	7.35	264.6
CCSD(T)/6-311G(2df)	6.13	259.6	6.68	246.5	6.51	262.3	6.84	265.9
CCSD(T,raw)/6-311G(2df)	6.18	258.9	6.74	245.3	6.56	261.5	6.89	265.2
MP2(full)/6-311G(d) geometry[c]								
MP2(full)/6-311G(d)	5.54	258.3	6.72	246.8	6.02	258.6	6.81	265.9

[a] Including ΔZPVE at the HF/6-31G(d) level scaled by 0.893.
[b] Including ΔZPVE at the B3LYP/6-311G(d) level.
[c] Including ΔZPVE at the MP2(full)/6-311G(d) level.

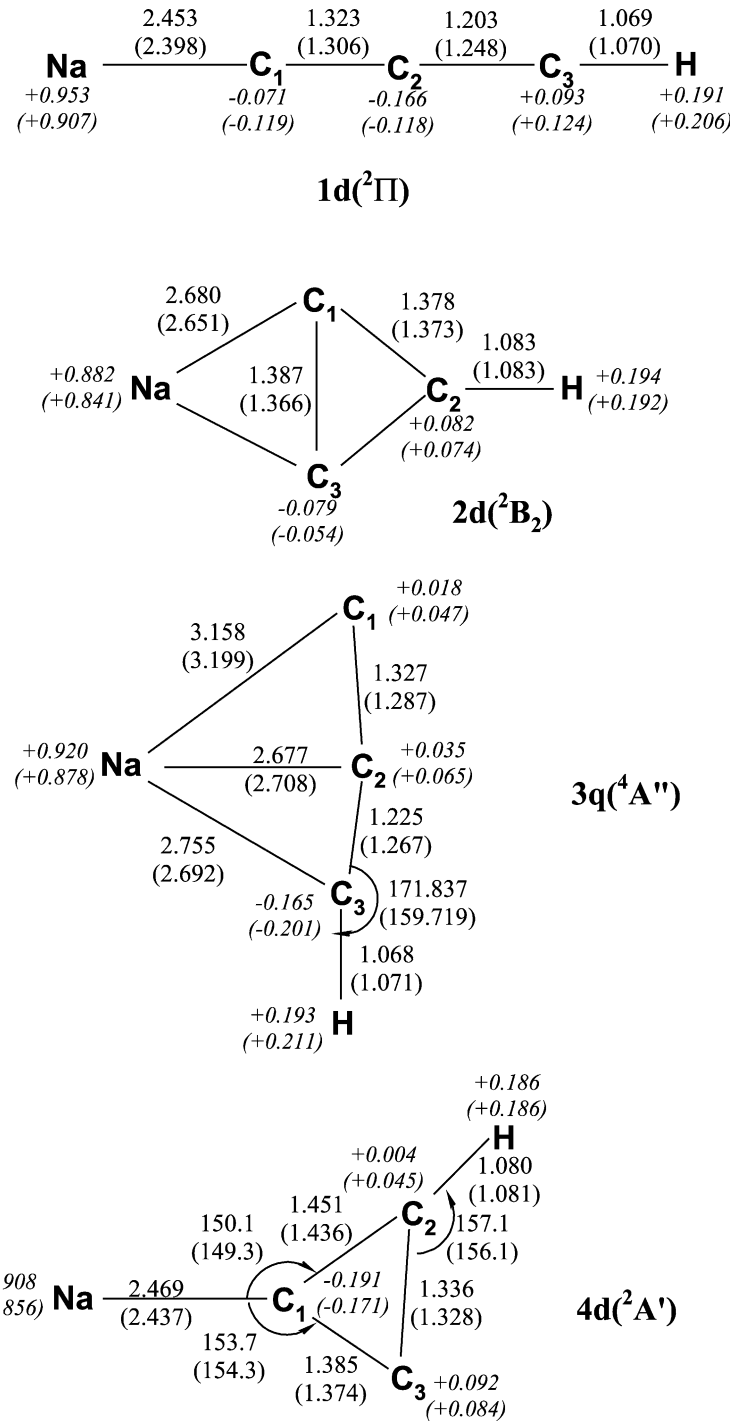

Fig. 2. MP2(full)/6-311G(d,p) and B3LYP/6-311G(d,p) (in parentheses) optimized geometries for the different NaC_3H^+ isomers. Distances are given in angstroms and angles in degrees. Effective Mulliken charges on atom (shown in italics) computed using HF/6-311G(d,p) and B3LYP/6-311G(d,p) (in parentheses) densities.

Table 5
MP2(full)/6-311G(d,p) and B3LYP/6-311G(d,p) (in parentheses) vibrational frequencies, in cm^{-1}, ZPV energies, in kcal/mol, and dipole moments, in Debyes, for the different NaC_3H^+ species

	1d ($^2\Pi$)	**2d** ($^2B_2$)	**3q** ($^4A''$)	**4d** ($^2A'$)
$\nu_1(a_1,\sigma,a')$	3510 (3400)	3298 (3236)	3470 (3364)	3323 (3256)
$\nu_2(a_1,\sigma,a')$	2168 (1914)	1637 (1624)	1730 (1706)	1649 (1665)
$\nu_3(a_1,\sigma,a')$	1268 (1277)	1186 (1213)	1170 (1276)	1276 (1242)
$\nu_4(a_1,\sigma,a')$	233 (251)	179 (181)	657 (530)	1055 (1050)
$\nu_5(b_2,\pi,a')$	1238 (885); 645 (440)	966 (943)	487 (441)	902 (897)
$\nu_6(b_2,\pi,a')$	474 (375); 363 (292)	121 (228)	187 (187)	233 (239)
$\nu_7(b_2,\pi,a')$	118 (116); 99 (106)	8164 (557i)	79 (47)	142 (144)
$\nu_8(b_1,\pi,a'')$		910 (887)	636 (449)	904 (898)
$\nu_9(b_1,\pi,a'')$		117 (117)	464 (357)	204 (211)
ZPVE	14.48 (12.95)	23.70 (12.06)	12.70 (11.95)	13.85 (13.73)
μ	5.446 (4.571)	4.914 (4.818)	6.660 (6.180)	5.549 (5.588)

consequence of the following two dominant valence-bond structures:

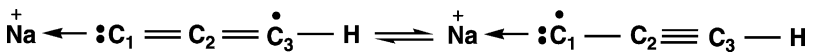

Protonation of isomer **1d** of NaC_3 keeps the linearity, and results in a shortening of the C_2-C_3 bond, whereas the C_1-C_2 bond distance is considerably lengthened. Structure **1d** can also be viewed as the result of the side interaction of a sodium cation with linear C_3H ($^2\Pi$). C–C and C–H bond distances are very close to that obtained for the hydrocarbon. This linear doublet isomer has all real frequencies and therefore corresponds to a true minimum on the potential surface. The IR intensities suggest that the infrared spectrum would be dominated by the ν_2 frequency corresponding to the C–C asymmetric stretching.

Structure **2** is obtained upon protonation at the unique carbon atom of the four-membered ring isomer of NaC_3 [24]. Protonation at one of the equivalent carbon atoms led to the **4d** isomer. The lowest-lying doublet ($^2B_2$), corresponding with the following electronic configuration:

$$\{\text{core}\}(6a_1)^2(7a_1)^2(3b_2)^2(8a_1)^2(2b_1)^2(9a_1)^2(4b_2)^1 \quad (6)$$

The unpaired electron is located at the C_3 unit and the positive charge at the sodium atom. The critical point data for isomer **2d**, presented in Table 6, show that there are bond critical points between C_1-C_2, C_2-C_3, C_3-C_1 and a $C_1C_2C_3$ ring critical point, therefore molecular topology suggests a truly three-membered ring. There are no individual Na–C bonds, since one bond critical point is found connecting Na^+ cation with the middle point of the C_1-C_3 bond. However, this structure can be considered as a π-interaction of Na^+ with a cyclic C_3H unit. As can be seen in Table 5, isomer **2d** has an imaginary b_2 mode, corresponding to the asymmetric stretching of C_3 unit, at the B3LYP level, whereas it is found to be unphysically large at the MP2 level. Our attempts to obtain true minima following the b_2 mode led to **4d** structure.

We have also optimized the $^2A_1$ state for structure **2** that corresponds to the lowest-lying doublet of NaC_3 isomer. This state is also a transition state at both MP2 and B3LYP levels and is placed approximately 7 kcal/mol higher in energy than the $^2B_2$ state.

Isomer **3** is obtained upon protonation of a T-shaped NaC_3 species at one of the equivalent carbon atoms. This isomer can also be viewed as the results of the side interaction of Na^+ with a linear C_3H ($^4\Sigma$) unit. We have searched for the corresponding doublet state, **3d**, but all our attempts collapsed into structure **1d**. The lowest-lying quartet ($^4A''$), namely **3q**, corresponds to

Table 6
Critical point data for NaC_3H^+ species, using the MP2(full)/6-311(d,p) and B3LYP/6-311G(d,p) (in parentheses) wave functions

Structure	Type	R^a (Å)	R^b (Å)	$\rho(r)$ (a.u.)	$\nabla^2\rho(r)$ (a.u.)	ε	$-H(r)$ (a.u.)
1d	Na–C_1 bond	2.452 (2.398)	2.452 (2.398)	0.0209 (0.0238)	0.1112 (0.1234)	0.0559 (0.0521)	0.0236 (0.0264)
	C_1–C_2 bond	1.323 (1.306)	1.323 (1.306)	0.3476 (0.3594)	−1.1342 (−1.1757)	0.0848 (0.1630)	0.1370 (0.1490)
	C_2–C_3 bond	1.203 (1.248)	1.203 (1.248)	0.4047 (0.3842)	−1.0397 (−1.1963)	0.0696 (0.0666)	0.3872 (0.2146)
	C_3–H bond	1.069 (1.070)	1.069 (1.070)	0.2916 (0.2880)	−1.1572 (−1.0852)	0.0672 (0.0475)	0.0259 (0.0261)
2d	Na–X[c] bond			0.0112 (0.0123)	0.0637 (0.0673)	2.3560 (2.2737)	0.0124 (0.0132)
	C_1–C_2 bond	1.377 (1.373)	1.378 (1.375)	0.2907 (0.2945)	−0.4790 (−0.4732)	0.8250 (0.8960)	0.1970 (0.1959)
	C_1–C_3 bond	1.387 (1.366)	1.389 (1.368)	0.3123 (0.3293)	−0.6761 (−0.7981)	0.4265 (0.3730)	0.1752 (0.1705)
	C_2–H bond	1.083 (1.083)	1.083 (1.083)	0.2837 (0.2853)	−1.0573 (−1.0503)	0.0122 (0.0129)	0.0291 (0.0237)
	$C_1C_2C_3$ ring			0.2670 (0.2732)	0.1477 (0.1600)		0.2522 (0.2543)
3q	Na–X[d] bond			0.0126 (0.0126)	0.0597 (0.0579)	0.5899 (0.7748)	0.0121 (0.0117)
	C_1–C_2 bond	1.327 (1.287)	1.327 (1.287)	0.3196 (0.3435)	−0.8724 (−0.9477)	0.0068 (0.0178)	0.1563 (0.1866)
	C_2–C_3 bond	1.225 (1.267)	1.226 (1.268)	0.3856 (0.3648)	−1.1103 (−1.0659)	0.0281 (0.0385)	0.2632 (0.2014)
	C_3–H bond	1.068 (1.071)	1.068 (1.071)	0.2829 (0.2810)	−1.0447 (−1.0004)	0.0008 (0.0020)	0.0352 (0.0330)
4d	Na–C_1 bond	2.469 (2.437)	2.470 (2.437)	0.0207 (0.0226)	0.1051 (0.1104)	0.0112 (0.0119)	0.0225 (0.0238)
	C_1–C_2 bond	1.451 (1.436)	1.467 (1.447)	0.2642 (0.2714)	−0.2754 (−0.3177)	1.1767 (1.0899)	0.1784 (0.1736)
	C_1–C_3 bond	1.385 (1.374)	1.392 (1.380)	0.3018 (0.3117)	−0.6458 (−0.7040)	0.3618 (0.3451)	0.1662 (0.1610)
	C_2–C_3 bond	1.336 (1.328)	1.347 (1.336)	0.3132 (0.3228)	−0.6965 (−0.7504)	0.2693 (0.2585)	0.1944 (0.1907)
	C_2–H bond	1.080 (1.081)	1.080 (1.081)	0.2827 (0.2847)	−1.0434 (−1.0389)	0.0203 (0.0211)	0.0313 (0.0256)
	$C_1C_2C_3$ ring			0.2555 (0.2612)	0.1613 (0.1861)		0.2393 (0.2435)

[a] Bond length.
[b] Bond path length.
[c] Middle point of the C_1–C_3 bond.
[d] Middle point of the C_2–C_3 bond.

the following electronic configuration:

$$\{\text{core}\}\ (8a')^2(9a')^2(10a')^2(2a'')^2(11a')^2(12a')^1(13a')^1(3a'')^1 \quad (7)$$

The results of the topological analysis of charge density (Table 6) show that the isomer **3q** is best described as a π-interaction between sodium cation and the C_2–C_3 bond. Interaction of sodium cation with the terminal carbon of linear C_3H ($^4\Sigma$), gives the quartet state of isomer **1**. This isomer has an imaginary frequency (π symmetry) at both the MP2 and B3LYP levels. All our attempts to obtain true minima at both levels following the corresponding normal mode with imaginary frequency led to **3q** structure. We can conclude that a σ-interaction of sodium cation with linear C_3H is most favorable on the doublet surface (isomer **1d**), whereas on the quartet surface π-interaction is the most stable (isomer **3q**). Isomer **3q** can be represented by the following valence-bond structures:

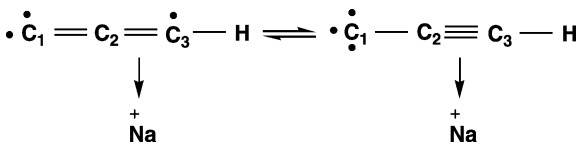

The positive charge resides in the sodium atom, two unpaired electrons are mainly located at the C_1 atom and the other one is distributed between C_1 and C_3. The C_1–C_2 bond distance is intermediate between typical double and single-bond lengths, and the C_2–C_3 value is also intermediate between a double and triple-bond. Both C–C bond distances are very similar to that found of the C_3H ($^4\Sigma$). As can be seen in Table 5, isomer **3q** has all real frequencies and therefore corresponds to a true minimum on the quartet potential surface.

Finally **4d** is obtained upon protonation of a three-membered ring NaC_3 isomer, and can also be viewed as the result of the interaction of Na^+ with a cyclic C_3H unit through an apex. The doublet state of this

isomer, $^2A'$, corresponds to the following electronic configuration:

$$\{\text{core}\}(8a')^2(9a')^2(10a')^2(11a')^2(2a'')^2(12a')^2(13a')^1 \quad (8)$$

The unpaired electron is located at the C_3 atom and the positive charge at the sodium. In contrast with neutral isomer, the topological analysis of the electronic charge density for isomer **4d** reveals a three-membered ring. This isomer represents a true minimum on the potential energy surface, since all its frequencies are real, as can be seen in Table 5. Four different vibrational frequencies ν_1, ν_4, ν_6 and ν_9, are predicted as the most intense lines in the IR spectrum at both MP2 and B3LYP levels.

In a previous study of the neutral NaC_3H system Petrie [25] has located three minima (I, II and III) on the singlet potential energy surface, corresponding to **2d**, **3q** and **1d** structures, respectively. In addition, he has also located two triplet states (IV and V) corresponding to **1d** and **4d** isomers, respectively. This study shows that structures I and II can be considered as π-complex of Na^+ with cyclic and linear C_3H^-, respectively, while II can be represented as a σ-complex of Na^+ with linear C_3H^-. The triplet isomer IV is best considered as a σ-complex of Na^+ and $CCCH^-$ (triplet), on the other hand, the dominant electronic component for isomer V is $[Na^- - C_3H^+]$. These descriptions explain the differences found between structures of neutral NaC_3H and cationic NaC_3H^+ systems.

As for NaC_3^+ system, the topological analysis of the electronic charge density shows that all Na–C bonds in NaC_3H^+ species should be classified as closed-shell interactions, corresponding essentially to electrostatics bonds. This fact is consistent with the positive partial charge of the sodium atom, which is always greater than +0.84 for all structures (Fig. 2). Sodium π-interactions (isomer **2d** and **3q**) have smaller values of $\rho(r)$ than σ-interactions (**1d** and **4d**) and consequently larger bond distances.

The Laplacian of the electronic charge density $\nabla^2\rho(r)$ has negative values for all C–C bond critical points, a sign characteristic of shared interactions. The highest value of $\rho(r)$ for carbon–carbon bonds is found for the C_2–C_3 of **1d** isomer that corresponds to the shortest C–C bond distance.

The relative energies of the different NaC_3H^+ species at different levels of theory, including ZPVE corrections, are shown in Table 7. We also provide the S^2 expectation values for the HF/6-311G(d,p) wave functions. In the case of B3LYP calculations, all S^2 values are very close to the exact value. We give the results at the same levels of theory that were shown for the NaC_3^+ (Table 3) and NaC_3 systems [24]. As a general trend it can be seen in Table 7 that for this system there is a very good agreement between G2(P) and CCSD(T) models. Also there is an excellent agreement between B3LYP and the corrected G2(P) results, with discrepancies lower than 2 kcal/mol, and give the same stability order. On the other hand MP2 seems unable to give reliable relative energies, and its performance does not improve significantly upon extension of the basis set. Finally, as in the case of NaC_3^+ system, inclusion of 2s, $2p_x$, $2p_y$ and $2p_z$ orbitals for sodium in the G2 and CCSD(T) calculations does not significantly modify their results.

For the NaC_3H^+ system, a linear isomer and a three-membered cyclic species lie quite close in energy. The most reliable levels of theory, namely G2(P) and CCSD(T), agree in the prediction of the linear isomer, **1d**, as the global minimum. The fact that isomer **1d** presents a certain degree of spin-contamination, made G2(P) values most reliable than G2 ones. Therefore, it is reasonably safe to predict **1d** as the global minimum of NaC_3H^+ system. Nevertheless, **4d** cannot be discarded as a possible candidate for experimental detection. The other doublet isomer, **2d**, (which is the transition state for the degenerate rearrangement of **4d**) lies about 10 kcal/mol above **4d**. Finally the quartet state, isomer **3q**, lies much higher in energy than the doublets. Compared with the neutral NaC_3H species [25], it is readily seen that ionization favors structures **1** and **4** over **2** and **3**. On the other hand, protonation of neutral NaC_3 system [24] retains the global minimum and stabilizes structure **4d** over **2d** and **3d**.

This system can be considered as the sodium substituted of the $C_3H_2^+$ hydrocarbon. A G2 study [40] for $C_3H_2^+$ has shown that the global minimum is the cyclic species similar to **4d**, with **1d** lying about 6.7 kcal/mol higher in energy. As in the case of NaC_3^+ system, NaC_3H^+ shows the same stability order than

Table 7
Relative energies (kcal/mol) for the NaC_3H^+ isomers at different levels of theory

	1d($^2\Pi$)	**2d**($^2B_2$)	**3q**($^4A''$)	**4d**($^2A'$)
MP2(full)/6-31G(d) geometry[a]				
MP2(full)/6-31(d)	0.0	−3.7	38.9	−13.1
G1	0.0	10.8	47.1	0.5
G2	0.0	9.6	46.6	−0.8
G2(thaw/MP2)	0.0	10.0	47.0	−0.8
G1(P)	0.0	16.6	47.7	6.6
G2(P)	0.0	15.5	47.1	5.3
B3LYP/6-311G(d,p) geometry[b]				
B3LYP/6-311G(d,p)	0.0	15.0	49.3	4.3
CCSD(T)/6-311G(2df,p)	0.0	10.7	43.5	0.6
CCSD(T,raw)/6-311G(2df,p)	0.0	11.0	43.6	0.7
MP2/6-311G(d,p) geometry[c]				
MP2/6-311G(d,p)	0.0	−4.2	38.8	−14.8
$\langle S^2\rangle$	0.973	0.779	4.068	0.768

[a] Including ΔZPVE at the HF/6-31G(d) level scaled by 0.893.
[b] Including ΔZPVE at the B3LYP/6-311G(d,p) level.
[c] Including ΔZPVE at the MP2(full)/6-311G(d,p) level.

the chlorine substituted system, HC_3Cl^+ [41]. However, the nature of the bonds (NaC and Cl–C) in these systems is very different.

We have calculated the dissociation energies for the different NaC_3H^+ species. We obtain a value of 31.5(28.4) kcal/mol (at the G2(thaw/MP2) and CCSD(T,raw) (in parentheses) levels, respectively) for the dissociation of isomer **1d** into $Na^+ + CCCH$ and a value of 27.4 (27.5) kcal/mol (at the G2(thaw/MP2) and CCSD(T,raw) (in parentheses) levels, respectively) for the dissociation energy of isomer **4d** into $Na^+ + c\text{-}C_3H$. These values show that NaC_3H^+ isomers are relatively stables upon dissociation.

The present calculations for NaC_3H^+ allow an estimate of the proton affinities for NaC_3 isomers. In Table 4 we present the proton affinities at different levels of theory for the most stable isomers of NaC_3. As can be seen, all theoretical levels provide very similar proton affinities. The lowest proton affinity corresponds to NaC_3 ($^2A_1$) (244.2 kcal/mol, at the G2(thaw/MP2) level), and the bigger was found for NaC_3 ($^2A'$) (262.9 kcal/mol, at the G2(thaw/MP2) level). In all cases proton affinities are relatively high if comparison is made with the values of some important interstellar molecules. For example, the proton affinities of H_2, CO and C_2H_2 are 100, 143 and 152 kcal/mol, respectively. Therefore NaC_3, if present, would react quite easily in proton-rich interstellar media to give the protonated species. The proton affinities calculated for the NaC_3 isomers are similar to those of NaC_3H reported by Petrie [25] although are lower than those of other sodium-containing molecules (the proton affinities of $NaCH_3$ and $NaNH_3$ are 277.7 and 278.3 kcal/mol, respectively).

4. Conclusions

A theoretical study of the NaC_3^+ and NaC_3H^+ systems has been carried out. Predictions for their geometries and vibrational frequencies have been made at both MP2 and B3LYP levels, whereas electronic energies have been computed at G2 and CCSD(T) levels. Both systems can be viewed as the results of the interaction of sodium cation with the C_3 and C_3H hydrocarbons, respectively. The results of the topological analysis of the electronic charge density show that all Na–C bonds should be classified as closed-shell interactions, corresponding essentially

to electrostatic bonds with a small degree of covalent character.

According to our calculations, the predicted global minimum for NaC_3^+ is the linear isomer in its singlet state (structure **1s** ($^1\Sigma$)). The other two singlet (**2s** ($^1A_1$) and **4s** ($^1A_1$)) are not true minima and lie higher in energy. The lowest-lying triplet state is a three-membered ring **3t** ($^3B_2$), followed by the corresponding triplet state of linear isomer **1t** ($^3\Pi$) lying about 27.1 and 40.7 kcal/mol higher in energy that the predicted global minimum at the G2(P) level, respectively. Concerning the protonated species, NaC_3H^+, there are two isomers that lie close in energy: a linear species, **1d** ($^2\Pi$ and a three-membered ring, **4d** ($^2A'$). The most reliable levels of theory employed predict that **1d** ($^2\Pi$) is the global minimum, whereas **4d** ($^2A'$) is predicted to lie 5.3 kcal/mol higher in energy at the G2(P) level. In any case it seems that both structures could be accessible to experimental detection. High dipole moments have been estimated for these systems that could facilitate their detection.

An important conclusion from our calculations is that, as in the case of NaC_3 species, the B3LYP method leads to rather good relative energy predictions, because in most of the cases the results are quite close to the most expensive G2 and CCSD(T) methods. This is an interesting result for the study of more complex system related to NaC_3.

The results for the NaC_3^+ and NaC_3H^+ species allow an estimate of the ionization potential and proton affinity of NaC_3 system. The ionization potential of low-lying NaC_3 states vary from 6.42 (**1d** ($^2\Pi$)) to 6.94 (**4d** ($^2A'$)). Calculated proton affinities are all relatively high (in the range 245.8 (**2d** ($^2A_1$))–264.8 (**4d** ($^2A'$))). Therefore, if present in the interstellar medium, NaC_3 should be easily ionized and would react quite easily to give the protonated species.

Acknowledgements

This research has been supported by the Ministerio de Educación y Cultura of Spain (DGICYT, Grant PB97-0399-C03-01) and by the Junta de Castilla y León (Grant VA18/00B).

References

[1] M. Guelin, R. Lucas, J. Cernicharo, Astron. Astrophys. 280 (1993) L19.
[2] L.M. Ziurys, A.J. Apponi, M. Guelin, J. Cernicharo, Astrophys. J. 445 (1995) L47.
[3] J. Cernicharo, M. Guelin, Astron. Astrophys. 183 (1987) L10.
[4] L.M. Ziurys, C. Savage, J.L. Highberger, A.J. Apponi, M. Guelin, J. Cernicharo, Astrophys. J. 564 (2002) L45.
[5] B.E. Turner, T.C. Steimle, W.L. Meerts, Astrophys. J. 426 (1994) L97.
[6] Y. Zhang, C.Y. Zhao, W.H. Fang, Z.H. Lu, J. Mol. Struct. (Theochem) 454 (1998) 31.
[7] S. Arulmozhiraja, P. Kolandaivel, O. Ohashi, J. Phys. Chem. A 103 (1999) 3073.
[8] P. Botschwina, R. Oswald, Z. Phys. Chem. 215 (2001) 393.
[9] A.J. Apponi, M.C. McCarthy, C.A. Gottlieb, P. Thaddeus, J. Chem. Phys. 111 (1999) 3911.
[10] V.D. Gordon, E.S. Nathan, A.J. Apponi, M.C. McCarthy, P. Thaddeus, P. Botschwina, J. Chem. Phys. 113 (2000) 5311.
[11] J.R. Flores, A. Largo, Chem. Phys. 140 (1990) 19.
[12] L.B. Knight, S.T. Cobranchi, J.O. Herlong, C.A. Arrington, J. Chem. Phys. 92 (1990) 5856.
[13] G.V. Chertihin, L. Andrews, P.R. Taylor, J. Am. Chem. Soc. 116 (1994) 3513.
[14] B. Ma, Y. Yamaguchi, H.F. Schaefer, Mol. Phys. 86 (1995) 1331.
[15] H.L. Yang, K. Tanaka, M. Ahinada, J. Mol. Struct. (Theochem) 422 (1998) 159.
[16] D.V. Lanzisera, L. Andrews, J. Phys. Chem. A 101 (1997) 9660.
[17] X. Zheng, Z. Wang, A. Tang, J. Phys. Chem. A 103 (1999) 9275.
[18] C. Barrientos, P. Redondo, A. Largo, Chem. Phys. Lett. 320 (2000) 481.
[19] S. Green, Chem. Phys. Lett. 112 (1984) 29.
[20] D.E. Woon, Astrophys. J. 456 (1996) 602.
[21] X.E. Zheng, Z.Z. Wang, A.C. Tang, J. Mol. Struct. (Theochem) 492 (1999) 79.
[22] P. Redondo, C. Barrientos, A. Largo, Chem. Phys. Lett. 335 (2001) 64.
[23] P.J. Bruna, F. Grein, J. Chem. Phys. 112 (2000) 10796.
[24] C. Barrientos, P. Redondo, A. Largo, Chem. Phys. Lett. 343 (2001) 563.
[25] S. Petrie, J. Mol. Struct. (Theochem) 429 (1998) 1.
[26] S. Petrie, Mon. Not. R. Astron. Soc. 302 (1999) 482.
[27] R. Krishnan, J.S. Binkley, R. Seeger, J.A. Pople, J. Chem. Phys. 72 (1980) 650.
[28] A.D. Becke, J. Chem. Phys. 98 (1993) 5648.
[29] L.A. Curtiss, K. Raghavachari, G.W. Trucks, J.A. Pople, J. Chem. Phys. 94 (1991) 7221.
[30] K. Raghavachari, G.W. Trucks, J.A. Pople, M. Head-Gordon, Chem. Phys. Lett. 157 (1989) 479.
[31] T.J. Lee, P.R. Taylor, Int. J. Quantum Chem. Symp. 23 (1989) 199.
[32] S. Petrie, J. Phys. Chem. A 102 (1998) 6138.
[33] M.J. Frisch, G.W. Trucks, H.B. Schlegel, G.E. Scuseria, M.A.

Robb, J.R. Cheeseman, V.G. Zakrzewski, J.A. Montgomery Jr., R.E. Stratmann, J.C. Burant, S. Dapprich, J.M. Millan, A.D. Daniels, K.N. Kudin, M.C. Strain, O. Farkas, J. Tomasi, V. Barone, M. Cossi, R. Cammi, B. Mennucci, C. Pomelly, C. Adamo, S. Clifford, J. Ochterski, G.A. Petersson, P.Y. Ayala, Q. Cui, K. Morokuma, D.K. Malick, A.D. Rabuck, K. Raghavachari, J.B. Foresman, J. Cioslowski, J.V. Ortiz, A.G. Baboul, B.B. Stefanov, G. Liu, A. Liashenko, P. Piskorz, I. Komaromi, R. Gomperts, R.L. Martin, D.J. Fox, T. Keith, M.A. Al-Laham, C.Y. Peng, A. Nanayakkara, C. Gonzalez, M. Challacombe, P.M.W. Gill, B. Johnson, W. Chen, M.W. Wong, J.L. Andres, C. Gonzalez, M. Head-Gordon, E.S. Replogle, J.A. Pople, GAUSSIAN 98, Gaussian Inc., Pittsburgh, PA, 1998.

[34] R.F.W. Bader, Atoms in Molecules. A Quantum Theory, Clarendon Press, Oxford, 1990.
[35] D. Cremer, E. Kraka, Croat. Chim. Acta 57 (1985) 1259.
[36] P.L.A. Popelier, Comp. Phys. Commun. 93 (1996) 212.
[37] P. Redondo, A. Largo, F. García, C. Barrientos, Int. J. Quantum Chem. 84 (2001) 660.
[38] C. Barrientos, P. Redondo, A. Largo, Int. J. Quantum Chem. 86 (2002) 114.
[39] P. Redondo, J.R. Redondo, C. Barrientos, A. Largo, Chem. Phys. Lett. 315 (1999) 224.
[40] M.W. Wong, L. Radom, J. Am. Chem. Soc. 115 (1993) 1507.
[41] P. Redondo, J.R. Redondo, A. Largo, J. Mol. Struct. (Theochem) 505 (2000) 221.